Citation: CPT Pharmacometrics Syst. Pharmacol. (2015) 4, 445–453; doi:10.1002/psp4.12005

ORIGINAL ARTICLE

Modeling Suggests a Mechanism of Synergy Between Hepatitis C Virus Entry Inhibitors and Drugs of Other Classes

P Padmanabhan and NM Dixit*

Hepatitis C virus (HCV) entry inhibitors (EIs) act synergistically with drugs targeting other stages of the HCV lifecycle. The origin of this synergy remains unknown. Here, we argue that the synergy may arise from the complementary activities of the drugs across cell subpopulations expressing different levels of HCV entry receptors. We employ mathematical modeling of viral kinetics *in vitro*, where cells with a distribution of entry receptor expression levels are exposed to HCV with or without drugs. The drugs act independently in each cell, as expected in the absence of underlying interactions. Yet, at the cell population level our model predicts that the drugs exhibit synergy. EIs effectively block infection of cells with low receptor levels. With high receptor levels, where EIs are compromised, other drugs are potent. This novel mechanism of synergy, arising at the cell population level may facilitate interpretation of drug activity and treatment optimization.
CPT Pharmacometrics Syst. Pharmacol. (2015) **4**, 445–453; doi:10.1002/psp4.12005; published online on 6 July 2015.

Study Highlights

WHAT IS THE CURRENT KNOWLEDGE ON THE TOPIC? ☑ Strong synergy has been observed between the numerous inhibitors targeting hepatitis C virus (HCV) entry and antiviral agents targeting other stages of the HCV lifecycle. The origin of the synergy remains poorly understood. • WHAT QUESTION DID THIS STUDY ADDRESS? ☑ We constructed a mathematical model of HCV viral kinetics *in vitro* to unravel the mechanism of synergy between the drugs. • WHAT THIS STUDY ADDS TO OUR KNOWLEDGE ☑ Our model demonstrates that heterogeneity of entry receptor expression levels across cells, leading to complementary activity of drugs across different cell subpopulations, can give rise to the observed synergy between the HCV entry inhibitors and drugs of other classes. Synergy may thus arise not only from molecular/intracellular level interactions between drugs but also from heterogeneities at the cell population level. • HOW THIS MIGHT CHANGE CLINICAL PHARMACOLOGY AND THERAPEUTICS ☑ The mechanism of synergy that we have identified may enable more accurate interpretation of drug efficacies in combination and facilitate rational optimization of treatment with HCV entry inhibitors.

Hepatitis C virus (HCV) entry into target cells involves the viral envelope proteins E1 and E2 and several cell surface receptors including scavenger receptor class B type 1 (SR-B1),[1] CD81,[2] tight-junction proteins claudin-1 (CLDN1)[3] and occludin (OCLN),[4] Niemann-Pick C1-Like 1 (NPC1L1),[5] and transferrin receptor 1 (Tfr1).[6] Additionally, host factors such as epidermal growth factor receptor (EGFR)[7], ephrin receptor A2 (EphA2),[7] and HRas[8] have been shown to modulate HCV entry. Entry inhibitors (EIs) targeting viral envelop proteins or host receptors have been able to prevent infection *in vitro* and in a mouse model[5–15] and present a promising new class of anti-HCV drugs. Indeed, two EIs, ITX 5061, which targets SR-B1, and erlotinib, which targets EGFR, are in clinical trials and several compounds targeting other aspects of the HCV entry process are in development.[16,17]

Recent studies have observed strong synergy between EIs and other classes of direct-acting antiviral agents (DAAs) or host-targeting agents (HTAs) that are in use or in clinical development.[9,18] The EIs investigated in these studies are monoclonal antibodies targeting CD81, CLDN1, or SR-B1, and small molecule inhibitors targeting SR-B1 (ITX 5061), EGFR (erlotinib), or EphA2 (dasatinib). The DAAs investigated are protease inhibitors (telaprevir, boceprevir, simeprevir, and danoprevir), an NS5A inhibitor (daclatasvir), and polymerase inhibitors (sofosbuvir and mericitabine). The HTAs investigated are a cyclophilin inhibitor (alisporivir) and pegylated interferon α.

Synergy implies that in combination lower drug dosages can yield the desired efficacy. Consequently, unraveling the mechanism(s) underlying this observed synergy assumes importance: it would facilitate the rational identification of optimal drug dosages that would maximize treatment response, yielding guidelines for the use of EIs in combination with other drugs. One possibility that may give rise to synergy between an EI and another drug is the existence of an interaction, as yet unknown, between the HCV entry process and the step of the HCV lifecycle targeted by the other drug. For instance, if blocking one of the entry receptors were also to affect viral replication via signaling downstream of the entry receptor, then synergy between EIs and viral polymerase inhibitors may arise. Such a possibility, however, appears unlikely because EIs display synergy with drugs from several classes and interactions between each

Department of Chemical Engineering, Indian Institute of Science, Bangalore, Karnataka, India. *Correspondence: NM Dixit (narendra@chemeng.iisc.ernet.in)
Received 10 April 2015; accepted 4 June 2015; published online on 6 July 2015. doi:10.1002/psp4.12005

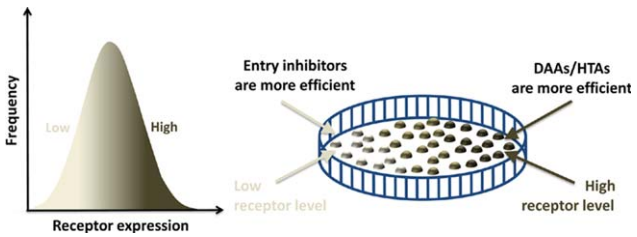

Figure 1 Schematic of the hypothesis. The expression level of an entry receptor varies across cells (left). The entry inhibitor is more effective in blocking the infection of cells with low receptor expression, whereas a DAA or an HTA of another class is more effective in blocking the infection of cells with high receptor expression (right). This complementary activity of the drugs across subpopulations of cells may give rise to synergy.

of the steps of the HCV lifecycle targeted by the latter drugs and the viral entry process are not foreseen. Another possibility is that EIs act on strains that carry resistance mutations to the other drug, thus increasing the overall genetic barrier of the combination. EIs, however, also exhibit synergy with interferon, which acts by stimulating the host-immune response, and against which resistant strains are not expected to arise. Thus, while the above mechanisms might contribute to synergy in specific cases, a more general mechanism appears to underlie the broadly observed synergy between EIs and other drugs.

Here we explore an alternative hypothesis that could explain the broad synergy between EIs and other drugs. We argue that synergy between an EI and another drug could arise from the complementary activities of the two drugs across cell subpopulations expressing different levels of entry receptors (**Figure 1**). By entry receptors we mean the cell or viral surface proteins or other host factors listed above that affect HCV entry. A distribution of the expression level of entry receptors is typically observed across cells in culture.[19] Entry efficiency increases with receptor expression.[19,20] Blocking virus entry into cells with higher receptor expression levels therefore requires larger dosages of the EI. Infection of such cells, however, can be blocked more readily by the other drug, which is unaffected by the efficiency of the entry process. Thus, when used in combination, the EI need only target cells with low entry receptor expression levels, which is accomplished at lower dosages, leading to the observed synergy.

To test this hypothesis, we constructed two mathematical models: a conceptual model that serves to elucidate the key underpinnings of the hypothesis, and a more comprehensive model that mimics experiments. We found, interestingly, that although, as expected, the drugs acted independently at the single-cell level, they displayed synergy at the cell-population level and that the extent of synergy increased with increase in the heterogeneity of entry receptor expression levels across cells.

METHODS

Conceptual model

Framework. We first constructed a simple, conceptual model where target cells, T, consisted of only two subpopulations, T_1 and T_2, with cells T_2 expressing more of a particular entry receptor than T_1 (**Figure 2a**). Otherwise, the cells were assumed to be identical. We let the cells be exposed to HCV virions, V, in the presence or absence of drugs. We assumed that the EI targeted the receptor that distinguished T_1 from T_2. Accordingly, the inhibitor blocked the infection of T_1 more efficiently than that of T_2. The other drug (a DAA or an HTA of another class) worked independently of the entry receptor and thus blocked the infection of T_1 and T_2 to the same extent. We constructed the following equations to describe the ensuing viral kinetics.

$$\frac{dT_i}{dt} = \lambda\left(1-\frac{T_1+T_2}{T_{\max}}\right)T_i-\mu T_i-\beta(1-\varepsilon_i)T_iV,\ \ i=1,2 \qquad (1)$$

$$\frac{dI_i}{dt} = \beta(1-\varepsilon_i)T_iV-\delta I_i,\ \ i=1,2 \qquad (2)$$

$$\frac{dV}{dt} = p(I_1+I_2)-cV \qquad (3)$$

Here, target cells proliferate and die with rate constants λ and μ, respectively. $T_{\max}$ is the carrying capacity of the cell culture and β is the second-order infection rate constant. Infection of target cells produces the respective infected cells I_i. Based on recent observations of HCV-induced cell cycle arrest *in vitro*, we neglected the proliferation of infected cells.[21,22] Infected cells die with an enhanced death rate constant δ due to HCV-induced cytopathicity *in vitro*.[23] Free virions are produced from each infected cell and are cleared, with rate constants p and c, respectively. When drugs are present, we assumed that infection is inhibited by blocking the infection of T_1 and T_2 with net efficacies ε_1 and ε_2, respectively. (We recognize that the other drug may lower viral production instead, but because viral production and clearance are rapid, the resulting pseudo-steady state,[20,24] $V \sim \frac{p(I_1+I_2)}{c}$, effectively translates to a lowering of infection; see **Supplementary Text**.)

Drug efficacies. We obtained ε_1 and ε_2 as follows. In the presence of the EI alone, we defined $\varepsilon_1 = \varepsilon_{E1}$ and $\varepsilon_2 = \varepsilon_{E2}$. We assumed the dose–response relationship of drugs to follow a Hill function. Accordingly, the EI at concentration C_E blocked the infection of T_1 and T_2 with the defined efficacies $\varepsilon_{E1} = \frac{(C_E)^{m_{E1}}}{(IC_{50}^{E1})^{m_{E1}}+(C_E)^{m_{E1}}}$ and $\varepsilon_{E2} = \frac{(C_E)^{m_{E2}}}{(IC_{50}^{E2})^{m_{E2}}+(C_E)^{m_{E2}}}$, respectively, where IC_{50}^{E1} and IC_{50}^{E2} are the drug concentrations of the EI required to block the infection of T_1 and T_2 by 50% and m_{E1} and m_{E2} are the Hill coefficients.

In the presence of the other drug alone, we let $\varepsilon_1 = \varepsilon_2 = \varepsilon_A$. The other drug at concentration C_A blocked the infection of both T_1 and T_2 with efficacy $\varepsilon_A = \frac{(C_A)^{m_A}}{(IC_{50}^{A})^{m_A}+(C_A)^{m_A}}$. Again, IC_{50}^{A} is the concentration of the other drug required to block the infection of both T_1 and T_2 by 50% and m_A is the Hill coefficient.

In the presence of both drugs, we assumed that the drugs acted independently within each subpopulation. Accordingly, we obtained ε_1 and ε_2 by setting the combination index (CI)[25] (defined below) to unity in both populations. We considered first the subpopulation T_1. The efficacy ε_1 when the EI at concentration C_E and the other

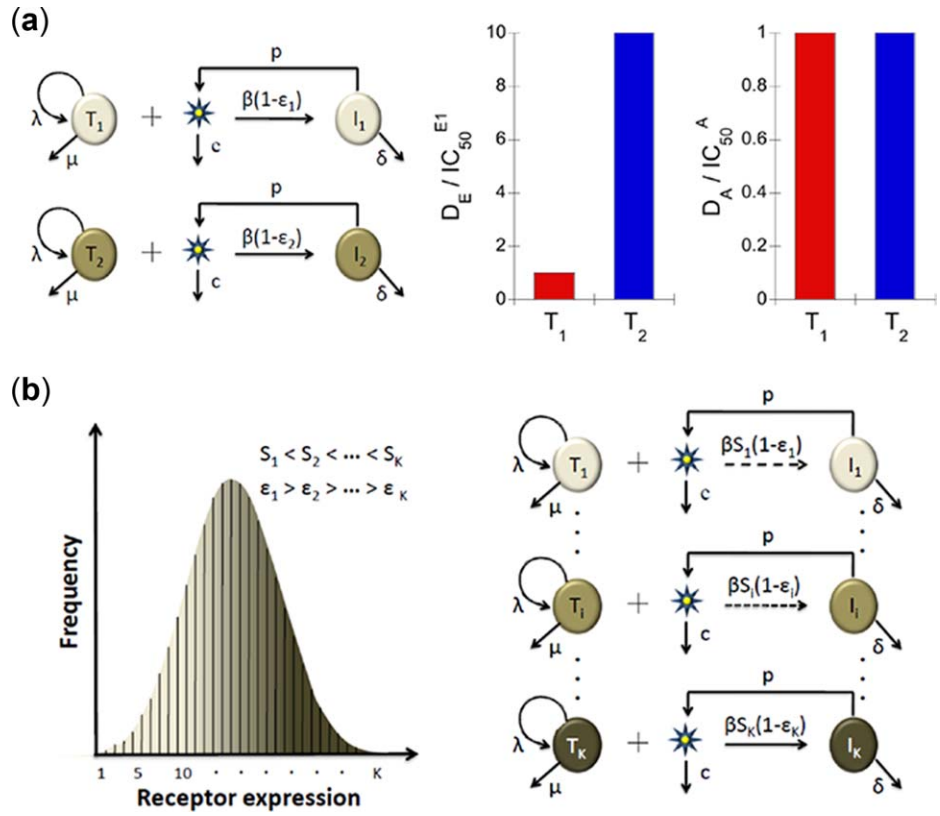

Figure 2 Schematic of the models. (**a**) Conceptual model of viral kinetics following exposure of target cells expressing two discrete levels of the entry receptor (low or high) to HCV virions (left). An entry inhibitor blocks the infection of receptor-low cells more effectively, whereas a DAA or an HTA of another class blocks the infection of cells independently of receptor expression (right). (**b**) Model of viral kinetics *in vitro* (right) following exposure of target cells with a distribution of the entry receptor expression level (left) to HCV virions. The dependence of susceptibility to infection on entry receptor expression, S_i, increases and the efficacy of entry inhibitors, ε_i, decreases with increase in the receptor expression level. The other symbols employed are defined in the **Methods**.

drug at concentration C_A are used together is given by enforcing independence based on *CI*:

$$\frac{C_E}{(C_E)_a}+\frac{C_A}{(C_A)_a}=1, \tag{4}$$

where $(C_E)_a$ and $(C_A)_a$ are concentrations of the EI and the other drug required to block the infection with the same efficacy ε_1 when they are used alone. Using $\varepsilon_1=\varepsilon_{E1}$ and $\varepsilon_1=\varepsilon_A$ in the dose–response relationships of the drugs above, it follows that $(C_E)_a=IC_{50}^{E1}(\frac{1}{\varepsilon_1}-1)^{-1/m_{E1}}$ and $(C_A)_a=IC_{50}^{A}(\frac{1}{\varepsilon_1}-1)^{-1/m_A}$. Substituting the latter expressions in Eq. 4 yielded

$$\frac{C_E}{IC_{50}^{E1}\left(\frac{1}{\varepsilon_1}-1\right)^{-1/m_{E1}}}+\frac{C_A}{IC_{50}^{A}\left(\frac{1}{\varepsilon_1}-1\right)^{-1/m_A}}=1 \tag{5}$$

solving which yielded ε_1 for the concentrations C_E and C_A employed. Similarly, solving the corresponding equation,

$$\frac{C_E}{IC_{50}^{E2}\left(\frac{1}{\varepsilon_2}-1\right)^{-1/m_{E2}}}+\frac{C_A}{IC_{50}^{A}\left(\frac{1}{\varepsilon_2}-1\right)^{-1/m_A}}=1 \tag{6}$$

yielded ε_2, the combined efficacy in the subpopulation T_2.

Using ε_1 and ε_2 thus obtained, Eqs. 1–3 can be solved to predict viral kinetics under exposure to any drug levels C_E and C_A given the initial distribution of the cell population into the two subpopulations. We assumed that at the start of the infection a fraction ϕ of the target cells is of type T_2. We varied ϕ between 0 and 1. Further, we assumed that infection was seeded by free virions and no infected cells existed at the start.

Synergy. The predictions of viral kinetics were employed to assess the synergy between the drugs. This involved solving the inverse problem of identifying drug concentrations for a desired level, x, of inhibition of infection at a fixed timepoint during the course of infection, with the inhibition measured in terms of the fraction of cells infected. We first fixed x to, say, 50%. We solved the model equations above first without drugs and predicted the number of infected cells at the desired timepoint, say, 3 days postinfection. We next solved the equations in the presence of the EI alone and identified that concentration $(C_E)_x$ at which the number of infected cells was lowered by the factor x at the desired timepoint. We repeated the procedure with the other drug alone and identified the corresponding concentration $(C_A)_x$. We finally solved the equations with the drugs used simultaneously and identified the concentrations C_E and C_A at

which the same level of inhibition was achieved. To minimize our search space, following experiments,[9,18] we let the ratio of C_E and C_A be equal to the ratio of $(C_E)_x$ and $(C_A)_x$; i.e., $C_E/C_A = (C_E)_x/(C_A)_x$. The combination index,

$$CI_x = \frac{C_E}{(C_E)_x} + \frac{C_A}{(C_A)_x}, \quad (7)$$

then yielded the extent of synergy (or antagonism) between the drugs at the level of inhibition considered. (Use of the alternative expression, $CI_x = \frac{C_E}{(C_E)_x} + \frac{C_A}{(C_A)_x} + \frac{C_E C_A}{(C_E)_x (C_A)_x}$, did not alter our findings; see **Supplementary Figure 1**.) We repeated the procedure for different values of x (=50%, 75% and 90%) as in the experiments.[9,18]

Model of HCV viral kinetics *in vitro*

Framework. We next considered *in vitro* experiments where a population of target cells is exposed to a population of HCV virions with or without drugs (**Figure 2b**). The cell population was assumed to exhibit a distribution of the expression level of the entry receptor above. We therefore divided the target cells into K subpopulations, denoted by T_i, where $i = 1, 2, \ldots, K$, with cells T_i expressing the entry receptor in a narrow range Δn_i around n_i molecules per unit area. The following equations describe the ensuing viral kinetics:

$$\frac{dT_i}{dt} = \lambda\left(1 - \frac{\sum_{i=1}^{K} T_i}{T_{\max}}\right) T_i - \mu T_i - \beta(1-\varepsilon_i) S_i T_i V, \;\; i = 1, 2, \ldots, K \quad (8)$$

$$\frac{dI_i}{dt} = \beta(1-\varepsilon_i) S_i T_i V - \delta I_i, \;\; i = 1, 2, \ldots, K \quad (9)$$

$$\frac{dV}{dt} = p\sum_{i=1}^{K} I_i - cV \quad (10)$$

Here, λ, μ, δ, p, c, and $T_{\max}$ are the same as in Eqs. 1–3. We additionally recognized that the efficiency of entry increases with the expression level of the entry receptor, n_i. We modeled this efficiency using the relative susceptibility S_i of cells T_i to virus entry. Based on previous studies,[20,26] we let S_i depend on entry receptor expression following a Hill function, $S_i = \frac{(n_i)^h}{(n_i^{50})^h + (n_i)^h}$, where h is the Hill coefficient and n_i^{50} is the entry receptor expression level at which $S_i = 0.5$. Note that when $n_i \approx 0$, $S_i \approx 0$ and when $n_i \gg n_i^{50}$, $S_i \approx 1$. β is thus the infection rate of cells expressing the entry receptor in excess.

Drug efficacies. Here we adopted a more mechanistic approach to evaluate the efficacy of the EI, based on the assumption that it targeted the entry receptor that distinguished the different cell subpopulations. (Note that the empirical approach based on the Hill function employed in the conceptual model above can also be used here.) In the presence of the inhibitor, thus, the number of free receptors, n_i^f, available for HCV entry decreased due to the formation of the receptor–inhibitor complexes, n_i^b. The susceptibility of cells T_i to infection in the presence of the EI consequently reduced to $S_i^d = \frac{(n_i^f)^h}{(n_i^{50})^h + (n_i^f)^h}$. Assuming complex formation to be rapid, we estimated the number of complexes formed using reaction equilibrium to be $n_i^b = \frac{n_i^f C_E}{K_D^E}$, where K_D^E is the equilibrium dissociation constant of the complexes. Mass balance on the receptor expression level, $n_i = n_i^f + n_i^b$, then yielded $n_i^b = \frac{C_E}{K_D^E + C_E} n_i$ and $n_i^f = \frac{K_D^E}{K_D^E + C_E} n_i$. Substituting the latter expression for n_i^f in the expression above yielded S_i^d. We recognized next that $S_i^d = S_i(1-\varepsilon_{Ei})$, where ε_{Ei} is the efficacy of the EI in cells T_i, when used alone. Using the expression for S_i^d, combining it with the expression for S_i and rearranging terms yielded ε_{Ei} as a function of the receptor expression level, n_i:

$$\varepsilon_{Ei} = \frac{\left(1 + \frac{C_E}{K_D^E}\right)^h - 1}{\left(1 + \frac{C_E}{K_D^E}\right)^h + \left(\frac{n_i}{n_i^{50}}\right)^h} \quad (11)$$

By letting $\varepsilon_{Ei} = 0.5$, we obtained from the above expression the concentration of the EI required to block the infection of T_i by 50%: $IC_{50}^{Ei} = K_D^E\left((2 + (\frac{n_i}{n_i^{50}})^h)^{1/h} - 1\right)$.

Like in the conceptual model, the other drug was assumed to block the infection of cells in each subpopulation with efficacy $\varepsilon_A = \frac{(C_A)^{m_A}}{(IC_{50}^A)^{m_A} + (C_A)^{m_A}}$, independently of the expression level of the entry receptor. (Relaxing this assumption by allowing the latter efficacy also to exhibit an independent distribution across cells led to greater synergy; see **Supplementary Text, Supplementary Figure 2**.)

In the presence of the EI alone, $\varepsilon_i = \varepsilon_{Ei}$. In the presence of the other drug alone, $\varepsilon_i = \varepsilon_A$. In the presence of both the drugs at concentrations C_E and C_A, respectively, the combined efficacy, ε_i, can be obtained by solving the equation below, derived following the same procedure employed for Eq. 5, i.e., by enforcing $CI = 1$:

$$\frac{C_E}{\left(\left(\frac{1}{1-\varepsilon_i} + \frac{\varepsilon_i n_i^h}{(1-\varepsilon_i)\left(n_i^{50}\right)^h}\right)^{1/h} - 1\right) K_D^E} + \frac{C_A}{IC_{50}^A\left(\frac{1}{\varepsilon_i} - 1\right)^{-1/m_A}} = 1 \quad (12)$$

Knowledge of the efficacies, ε_i, allowed us to solve Eqs. 8–10 and predict the resulting viral kinetics for any C_E and C_A given an initial distribution of cells in the various subpopulations.

Synergy. To estimate synergy, we followed the same procedure employed in the conceptual model above, where we first identified the concentrations $(C_E)_x$ and $(C_A)_x$ of the EI and the other drug required for achieving a desired level of inhibition, x, when used alone. We then determined the concentrations C_E and C_A at which the same level of inhibition was achieved when the drugs were used together. CI, evaluated using Eq. 7, then provided a measure of synergy.

Data

We considered data from previous cell culture studies where human hepatoma-derived cells were exposed to cell culture-derived HCVcc virions in the presence of EIs and/or

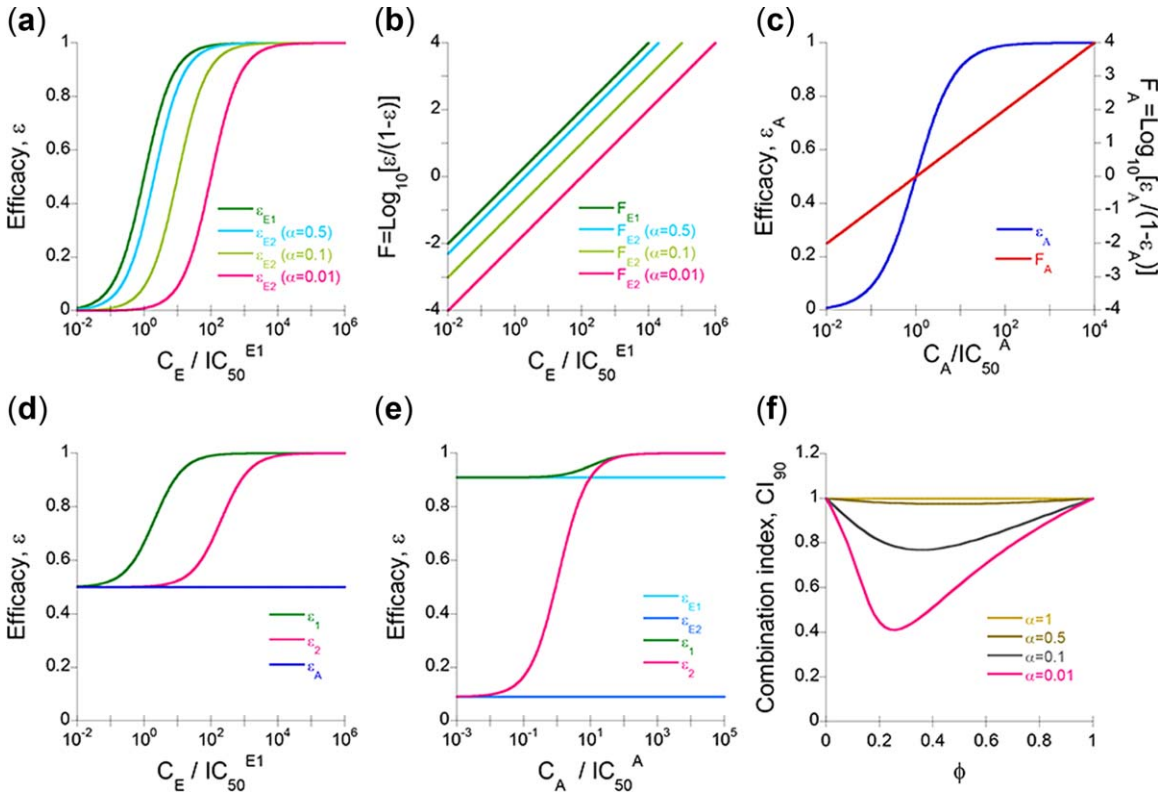

Figure 3 Predictions of the conceptual model. (**a**) The efficacy of the entry inhibitor, ε_{E1} and ε_{E2}, in blocking the infection of cells T_1 and T_2, respectively, for different entry inhibitor concentrations, C_E, and (**b**) the corresponding median-effect plot. ε represents the fraction of infection events prevented by the drug. The corresponding median effect equation, $F = \log_{10}\left(\frac{\varepsilon}{1-\varepsilon}\right)$, yields F as the logarithm of the ratio of the number of infection events inhibited by the drug to the number uninhibited. (**c**) The efficacy of a DAA or an HTA in blocking the infection of cells T_1 and T_2, ε_A, for different drug concentrations, C_A, and the corresponding median-effect plot. The efficacy of the combination in blocking the infections of T_1 and T_2, ε_1 and ε_2, (**d**) for fixed C_A ($= IC_{50}^{A}$) and different C_E and (**e**) for fixed C_E ($= 10IC_{50}^{E1}$) and different C_A. (**f**) Combination index, CI, determined at 90% inhibition of the cumulative level of infection at day 3 postinfection for different values of ϕ, the fraction of cells expressing high receptor expression levels, T_2, and α, the ratio of IC_{50}^{E1} and IC_{50}^{E2}. Drug concentrations are normalized by the respective IC_{50} values. Parameter values[20]: $\lambda = 0.44$ d^{-1}; $\mu = 1.7 \times 10^{-4}$ d^{-1}; $\delta = 1.1 \times 10^{-2}$ d^{-1}; $\beta = 1.2 \times 10^{-4}$ ml·(ffu·d)$^{-1}$; $p = 2.78$ ffu·(ml·d)$^{-1}$; and $c = 23.2$ d^{-1}. We assumed $T_{\max} = 7\times10^6$ cells · ml^{-1}, representative of *in vitro* cultures.[45] The Hill coefficients, $m_A = 1$, $m_{E1} = 1$ and $m_{E2} = 1$. In (**d**) and (**e**), $\alpha = 0.01$. Initial conditions: target cells, $T(0) = 10^5$ cells · ml^{-1}, with $T_1(0) = (1-\phi)T(0)$ and $T_2(0) = \phi T(0)$; virions, $V(0) = 10^5$ ffu · ml^{-1} (ffu stands for focus-forming units); and infected cells, $I_i(0) = 0$.

DAAs and HTAs of other classes. In these experiments, target cells proliferate, die, and get infected by HCVcc virions. Free virions are in turn produced by infected cells and are lost due to natural degradation. Viral infection was assessed using luciferase activity and *CI* was calculated at 50, 75, and 90% inhibition to assess synergy.[9,18]

Calculations and model parameters

We solved the model equations using computer programs written in MatLab (MathWorks, Natick, MA) and/or Berkeley Madonna (www.berkeleymadonna.com) and computed the time-evolution of all of the subpopulations of uninfected cells, T_i, infected cells, I_i, and the viral titer, V. The extent of inhibition was obtained as the ratio of the total population of infected cells, $I = \sum_{i=1}^{K} I_i$, in the presence of drug(s) to that in the absence of drugs at day 3 postinfection. Using viral load instead of infected cells to quantify the extent of inhibition did not alter our findings (**Supplementary Figure 3**). We employed model parameters that described the kinetics of infection of Huh-7.5 cells with JFH1 virus[20] (**Figure 3**). We also examined the sensitivity of our model predictions to variations in these parameter values (**Supplementary Figure 4**).

RESULTS

Conceptual model

To elucidate the role of heterogeneity in receptor expression in the observed synergy between an EI and a drug of another class, we constructed a conceptual model where target cells in culture expressed one of two discrete levels (high or low) of one entry receptor and were identical otherwise (**Figure 2a**; **Methods**). Within each cell, and hence subpopulation, we assumed that the drugs acted independently and examined whether they exhibited synergy at the cell population level by computing the combination

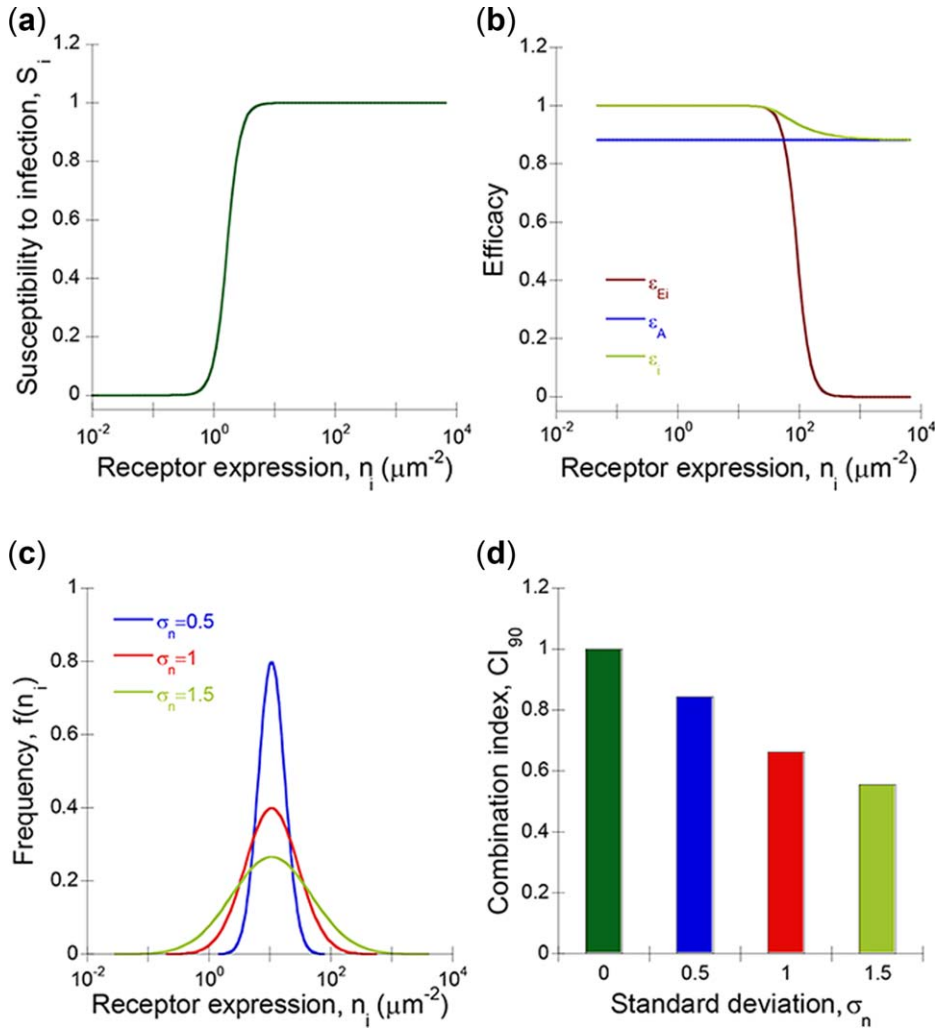

Figure 4 Predictions of the model of HCV kinetics *in vitro*. (**a**) Dependence of the susceptibility of a cell to infection, S_i, on its receptor expression level, n_i. (**b**) Efficacy of the entry inhibitor, ε_{Ei}, and the other drug, ε_A, and the combined efficacy of the two drugs, ε_i, as functions of n_i. (**c**) The log-normal distribution, $f(n_i) = \frac{1}{n_i \sigma_n \sqrt{2\pi}} e^{-\frac{(\ln n_i - \overline{n})^2}{2\sigma_n^2}}$, of the receptor expression level across cells, where $\overline{n}$ is the mean and σ_n is the standard deviation of $\ln n_i$. (**d**) Combination index, CI, determined at 90% inhibition of the cumulative level of infection at day 3 postinfection for different values of σ_n. The concentrations of the entry inhibitor and the other drug are normalized by K_D^E and IC_{50}^A, respectively. (Note that IC_{50}^{Ei} is directly proportional to K_D^E; see **Methods**.) Parameters: $m_A = 1$, $h = 4$, $\overline{n} = 2.9$ and $n_i^{50} = 1.65\,\mu m^{-2}$. In (b) $C_E = 54.77 K_D^E$ and $C_A = 7.47 IC_{50}^A$. Initial conditions: The fraction, $f(n_i)\Delta n_i$, of target cells belonging to the subpopulation T_i follow the log-normal distribution above. The other parameters and initial conditions are the same as those listed in **Figure 3**.

index (CI). $CI < 1$, $CI = 1$ and $CI > 1$ indicate synergy, additivity, and antagonism, respectively.

Efficacy of individual drugs. In the two cell subpopulations, denoted T_1 and T_2, the EI acted with different efficacies. The difference in the receptor expression level between the two subpopulations was assumed to affect the IC_{50}; specifically, $IC_{50}^{E1} < IC_{50}^{E2}$, indicating greater efficacy of the inhibitor in the subpopulation T_1 (**Figure 2a**). The efficacies in the two subpopulations, denoted ε_{E1} and ε_{E2}, respectively, increased with drug concentration in a sigmoidal manner (**Figure 3a**) (yielding a linear median-effect curve (**Figure 3b**). Further, as IC_{50}^{E2} increased relative to IC_{50}^{E1}, higher drug levels were required to achieve the desired ε_{E2}.

The dose–response curve of the other drug (a DAA or HTA of another class) also followed a sigmoidal pattern, but was the same for the two cell subpopulations (**Figures 2a**, **3c**).

Efficacy of drugs in combination. We examined next the combined effect of the two drugs in each cell subpopulation. The independent activities of the drugs implied that in each subpopulation $CI = 1$. Thus, for a range of concentrations of the EI, C_E, and a fixed concentration of the other drug, C_A, we computed the net efficacy ε_1 of the combination in the

subpopulation T_1, using Eq. 5 above. When C_E was small, $\varepsilon_1 \approx \varepsilon_A$, the efficacy corresponding to C_A alone (**Figure 3d**). As C_E increased, ε_1 rose in a sigmoidal manner and reached 1. For the subpopulation T_2, we found that much higher values of C_E were required to achieve the same efficacies as in T_1 (**Figure 3d**). The activity of the EI was thus more prominent in the subpopulation T_1. We repeated the calculations for fixed C_E and a range of values of C_A (**Figure 3e**). In the subpopulation T_1, $\varepsilon_1 \approx \varepsilon_{E1}$, the efficacy corresponding to C_E alone, when C_A was small and increased to 1 for large values of C_A. The trend was similar in the subpopulation T_2. However, the influence of the other drug was evident at much lower values of C_A in T_2 than in T_1; ε_2 began to rise above ε_{E2} at nearly 10-fold lower C_A than when ε_1 began to rise above ε_{E1}. The influence of the other drug was thus more prominent in the subpopulation T_2.

Synergy. To describe the scenario when both types of cells, T_1 and T_2, were present in culture, we solved the viral kinetics equations (Eqs. 1–3) using the efficacies illustrated above, and estimated the drug levels required to achieve 90% inhibition of infection at day 3 postinfection. The drug levels then yielded *CI* (via Eq. 7). We performed calculations over a range of values of ϕ ($0 \leq \phi \leq 1$), the fraction of cells of type T_2 at the start of infection, and different ratios of IC_{50}^{E1} and IC_{50}^{E2}, denoted by α (**Figure 3f** and **Supplementary Figure 5**). When ϕ was either 0 or 1, a single cell type existed in the population and *CI* equaled unity, indicating independence between the drugs. For intermediate values of ϕ, where the cell population was heterogeneous, *CI* was smaller than 1, indicating synergy. Similarly, when α was 1, indicating that the EI worked identically in the two subpopulations, heterogeneity was again lost and $CI = 1$ for all values ϕ. As α decreased, indicating greater distinction between the two subpopulations, *CI* decreased, indicating greater synergy between the drugs. Our model thus predicted synergy between the drugs ($CI < 1$) as arising from the heterogeneity of the underlying cell population and the resulting complementary activity of the drugs across cells.

With this conceptual understanding, we examined next whether a model that mimicked *in vitro* studies with cells exhibiting a continuous distribution of receptor expression levels also displayed synergy due to the same underlying principle.

Model of HCV viral kinetics *in vitro*

We divided target cells into several subpopulations with distinct receptor expression levels (**Figure 2b**) to mimic the distribution of receptor expression levels observed in cell culture studies. Further, we allowed entry efficiency to depend on receptor expression and estimated EI efficacy by quantifying its ability to block the entry receptor in question. The efficacy of the other drug remained independent of receptor expression. In each cell, the action of the two drugs was again assumed to be independent of each other. We estimated *CI* based on a desired level of inhibition at different times postinfection to assess synergy at the cell population level (**Methods**).

Drug efficacies. The susceptibility of a cell to infection increased with receptor expression in a sigmoidal manner (**Figure 4a**). The efficacy of the EI correspondingly decreased with increase in receptor expression (**Figure 4b**). The efficacy of the other drug remained constant across subpopulations. We defined the combined efficacy of the drugs within each subpopulation, ε_i, to be independent (by letting $CI = 1$). ε_i showed a dependence on receptor expression, n_i, as follows (**Figure 4b**). When n_i was small, the EI was highly efficacious and more potent than the other drug. ε_i was then close to the efficacy of the EI. When n_i was large, the EI was compromised, whereas the other drug continued to exert its antiviral activity. ε_i was then well approximated by the efficacy of the latter drug. At intermediate n_i, ε_i gradually switched between the two extremes (**Figure 4b**).

Heterogeneity in receptor expression and synergy. With the above estimates of ε_i, we solved model equations (Eqs. 8–10) to predict the effect of drugs on HCV viral kinetics *in vitro* (**Supplementary Figure 6**) and estimated *CI*. (Note that the model equations are consistent with *in vitro* data of viral kinetics.[20,26]) We considered different levels of heterogeneity in the receptor expression level: as σ_n, the standard deviation of the log-normal distribution of receptor expression levels, increased, heterogeneity in receptor expression across cells increased (**Figure 4c**).

We found that *CI* remained equal to 1 when the receptor expression across cells was homogeneous ($\sigma_n = 0$) (**Figure 4d**). This followed from the independence of the activities of the drugs in individual cells. We found, interestingly, that when the receptor expression across cells became heterogeneous ($\sigma_n > 0$), *CI* became less than 1, suggesting synergy. *CI* decreased as the heterogeneity in receptor expression (σ_n) increased (**Figure 4d**) as the complementary activity of the drugs at the population level became more prominent, consistent with our conceptual model (**Figure 3f**). *CI* was largely insensitive to model parameters (**Supplementary Figure 4**) or the time postinfection when the assessment of synergy is made (**Supplementary Figure 7**). Our prediction of synergy due to heterogeneity in receptor expression is thus robust to changes in model parameter values.

DISCUSSION

Recent studies have shown strong synergy between EIs and DAAs or HTAs of other classes.[9,18] Unraveling the mechanism of this observed synergy may facilitate optimization of combination treatments involving EIs. Mathematical models of HCV viral kinetics have been employed successfully to determine the effectiveness of treatment,[24,27–29] identify mechanisms of the action of drugs,[30,31] and to analyze patient data[24,27] and cell culture experiments.[20,26,32,33] In this study, advancing a previously developed mathematical model of HCV viral kinetics *in vitro*[20,26] to account explicitly for drug action, we suggest that heterogeneity of receptor expression across cells and the resulting complementary action of drugs across distinct

cell subpopulations may underlie the synergy between EIs and other drugs.

Synergy between drugs is thought to arise from an underlying interaction between the drugs or between the processes, pathways, and/or molecules they target.[34] For instance, we demonstrated recently that DAAs targeting viral replication can alter the systems-level properties of the interferon signaling network and improve responsiveness of cells to type I interferon.[28] Our current study presents an alternative explanation of the observed synergy between EIs and drugs of other classes based not on interactions between the drugs but on their complementary activities at the cell population level. Whereas EIs are likely to be more effective in blocking infection of cells with low entry receptor expression levels, the other drugs, whose effectiveness is independent of the entry receptor expression level, are expected to block the infection of cells with high entry receptor expression levels, bringing about synergy. Experiments that measure the effectiveness of drugs as a function of entry receptor expression levels would provide tests of our proposed explanation.

HCV entry into target cells can occur by cell-free virions or cell-to-cell transmission.[16,17] Although in our model we explicitly considered entry by cell-free virions, the model is applicable to entry via both modes.[20] The viral titer is typically proportional to the population of infected cells, so that the infection rate constant in our model can be thought of as an effective rate constant for infection by both modes. We recognize, however, that if the EI considered blocks entry by one mode alone, then entry by the other mode can predominate, compromising drug efficacy and the resulting synergy.[35]

The mode of synergy elucidated by our study may have broader applicability. We anticipate this mode of synergy to arise whenever two drugs target different molecules that exhibit distributions of their expression levels across cells and/or viral particles, allowing complementary activity of the drugs at the cell population level. Variations in the expression levels of molecules are intrinsic to cells.[36,37] Viral envelope proteins and other enzymes are also expected to exhibit intrinsic variations in expression levels.[38] This heterogeneity could thus explain at least in part the observed synergy between small molecule inhibitors of different HCV targets in recent *in vitro* studies,[39–41] between EIs targeting different aspects of the HCV entry process,[10,18,42,43] and perhaps also between several anti-HIV drugs.[44] Accounting for this new mode of synergy may be important for accurate quantification of drug action and rational treatment optimization.

Acknowledgment. This work was supported by the Department of Biotechnology Centre of Excellence for Research on Hepatitis C Virus, India and by the Department of Science and Technology, Government of India.

Conflict of Interest. The authors declare no conflicts of interest.

Author Contributions. P.P. and N.M.D. wrote the article; P.P. and N.M.D. designed the research; P.P. performed the research; P.P. and N.M.D. analyzed the data; P.P. and N.M.D. contributed new reagents/analytical tools.

1. Scarselli, E. *et al.* The human scavenger receptor class B type I is a novel candidate receptor for the hepatitis C virus. *EMBO J.* **21**, 5017–5025 (2002).
2. Pileri, P. *et al.* Binding of hepatitis C virus to CD81. *Science* **282**, 938–941 (1998).
3. Evans, M.J. *et al.* Claudin-1 is a hepatitis C virus co-receptor required for a late step in entry. *Nature* **446**, 801–805 (2007).
4. Ploss, A. *et al.* Human occludin is a hepatitis C virus entry factor required for infection of mouse cells. *Nature* **457**, 882–886 (2009).
5. Sainz, B., Jr. *et al.* Identification of the Niemann-Pick C1-like 1 cholesterol absorption receptor as a new hepatitis C virus entry factor. *Nat. Med.* **18**, 281–285 (2012).
6. Martin, D.N. & Uprichard, S.L. Identification of transferrin receptor 1 as a hepatitis C virus entry factor. *Proc. Natl. Acad. Sci. USA* **110**, 10777–10782 (2013).
7. Lupberger, J. *et al.* EGFR and EphA2 are host factors for hepatitis C virus entry and possible targets for antiviral therapy. *Nat. Med.* **17**, 589–595 (2011).
8. Zona, L. *et al.* HRas signal transduction promotes hepatitis C virus cell entry by triggering assembly of the host tetraspanin receptor complex. *Cell Host Microbe* **13**, 302–313 (2013).
9. Zhu, H. *et al.* Evaluation of ITX 5061, a scavenger receptor B1 antagonist: resistance selection and activity in combination with other hepatitis C virus antivirals. *J. Infect. Dis.* **205**, 656–662 (2012).
10. Fofana, I. *et al.* Monoclonal anti-claudin 1 antibodies prevent hepatitis C virus infection of primary human hepatocytes. *Gastroenterology* **139**, 953–964 (2010).
11. Meuleman, P. *et al.* Anti-CD81 antibodies can prevent a hepatitis C virus infection in vivo. *Hepatology* **48**, 1761–1768 (2008).
12. Lacek, K. *et al.* Novel human SR-BI antibodies prevent infection and dissemination of HCV in vitro and in humanized mice. *J. Hepatol.* **57**, 17–23 (2012).
13. Meuleman, P. *et al.* A human monoclonal antibody targeting scavenger receptor class B type I precludes hepatitis C virus infection and viral spread in vitro and in vivo. *Hepatology* **55**, 364–372 (2012).
14. Fafi-Kremer, S. *et al.* Viral entry and escape from antibody-mediated neutralization influence hepatitis C virus reinfection in liver transplantation. *J. Exp. Med.* **207**, 2019–2031 (2010).
15. de Jong, Y.P. *et al.* Broadly neutralizing antibodies abrogate established hepatitis C virus infection. *Sci. Transl. Med.* **6**, 254ra129 (2014).
16. Fofana, I., Jilg, N., Chung, R.T. & Baumert, T.F. Entry inhibitors and future treatment of hepatitis C. *Antiviral Res.* **104**, 136–142 (2014).
17. Zeisel, M.B., Lupberger, J., Fofana, I. & Baumert, T.F. Host-targeting agents for prevention and treatment of viral hepatitis C–perspectives and challenges. *J. Hepatol.* **58**, 375–384 (2013).
18. Xiao, F. *et al.* Synergy of entry inhibitors with direct-acting antivirals uncovers novel combinations for prevention and treatment of hepatitis C. *Gut* **64**, 483–494 (2014).
19. Koutsoudakis, G., Herrmann, E., Kallis, S., Bartenschlager, R. & Pietschmann, T. The level of CD81 cell surface expression is a key determinant for productive entry of hepatitis C virus into host cells. *J. Virol.* **81**, 588–598 (2007).
20. Padmanabhan, P. & Dixit, N.M. Mathematical model of viral kinetics in vitro estimates the number of E2-CD81 complexes necessary for hepatitis C virus entry. *PLoS Comput. Biol.* **7**, e1002307 (2011).
21. Walters, K.A. *et al.* Genomic analysis reveals a potential role for cell cycle perturbation in HCV-mediated apoptosis of cultured hepatocytes. *PLoS Pathog.* **5**, e1000269 (2009).
22. Kannan, R.P., Hensley, L.L., Evers, L.E., Lemon, S.M. & McGivern, D.R. Hepatitis C virus infection causes cell cycle arrest at the level of initiation of mitosis. *J. Virol.* **85**, 7989–8001 (2011).
23. Zhong, J. *et al.* Persistent hepatitis C virus infection in vitro: coevolution of virus and host. *J. Virol.* **80**, 11082–11093 (2006).
24. Neumann, A.U. *et al.* Hepatitis C viral dynamics in vivo and the antiviral efficacy of interferon-alpha therapy. *Science* **282**, 103–107 (1998).
25. Chou, T.C. Theoretical basis, experimental design, and computerized simulation of synergism and antagonism in drug combination studies. *Pharmacol. Rev.* **58**, 621–681 (2006).
26. Padmanabhan, P. & Dixit, N.M. Viral kinetics suggests a reconciliation of the disparate observations of the modulation of claudin-1 expression on cells exposed to hepatitis C virus. *PLoS ONE* **7**, e36107 (2012).
27. Rong, L., Dahari, H., Ribeiro, R.M. & Perelson, A.S. Rapid emergence of protease inhibitor resistance in hepatitis C virus. *Sci. Transl. Med.* **2**, 30ra32 (2010).
28. Padmanabhan, P., Garaigorta, U. & Dixit, N.M. Emergent properties of the interferon-signalling network may underlie the success of hepatitis C treatment. *Nat. Commun.* **5**, 3872 (2014).
29. Guedj, J. *et al.* Analysis of hepatitis C viral kinetics during administration of two nucleotide analogues: sofosbuvir (GS-7977) and GS-0938. *Antivir. Ther.* **19**, 211–220 (2013).
30. Dixit, N.M., Layden-Almer, J.E., Layden, T.J. & Perelson, A.S. Modelling how ribavirin improves interferon response rates in hepatitis C virus infection. *Nature* **432**, 922–924 (2004).

31. Guedj, J., Dahari, H., Pohl, R.T., Ferenci, P. & Perelson, A.S. Understanding silibinin's modes of action against HCV using viral kinetic modeling. *J. Hepatol.* **56**, 1019–1024 (2012).
32. Dahari, H., Sainz, B., Jr., Perelson, A.S. & Uprichard, S.L. Modeling subgenomic hepatitis C virus RNA kinetics during treatment with alpha interferon. *J. Virol.* **83**, 6383–6390 (2009).
33. Binder, M. *et al.* Replication vesicles are load- and choke-points in the hepatitis C virus lifecycle. *PLoS Pathog.* **9**, e1003561 (2013).
34. Fitzgerald, J.B., Schoeberl, B., Nielsen, U.B. & Sorger, P.K. Systems biology and combination therapy in the quest for clinical efficacy. *Nat. Chem. Biol.* **2**, 458–466 (2006).
35. Barretto, N., Sainz, B., Jr., Hussain, S. & Uprichard, S.L. Determining the involvement and therapeutic implications of host cellular factors in hepatitis C virus cell-to-cell spread. *J. Virol.* **88**, 5050–5061 (2014).
36. Niepel, M., Spencer, S.L. & Sorger, P.K. Non-genetic cell-to-cell variability and the consequences for pharmacology. *Curr. Opin. Chem. Biol.* **13**, 556–561 (2009).
37. Altschuler, S.J. & Wu, L.F. Cellular heterogeneity: do differences make a difference? *Cell* **141**, 559–563 (2010).
38. Pang, Y., Song, H., Kim, J.H., Hou, X. & Cheng, W. Optical trapping of individual human immunodeficiency viruses in culture fluid reveals heterogeneity with single-molecule resolution. *Nat. Nanotechnol.* **9**, 624–630 (2014).
39. Grunberger, C., Wyles, D.L., Kaihara, K.A. & Schooley, R.T. 3-drug synergistic interactions of small molecular inhibitors of hepatitis C virus replication. *J. Infect. Dis.* **197**, 42–45 (2008).
40. Wyles, D.L., Kaihara, K.A. & Schooley, R.T. Synergy of a hepatitis C virus (HCV) NS4A antagonist in combination with HCV protease and polymerase inhibitors. *Antimicrob. Agents Chemother.* **52**, 1862–1864 (2008).
41. Wyles, D.L., Kaihara, K.A., Vaida, F. & Schooley, R.T. Synergy of small molecular inhibitors of hepatitis C virus replication directed at multiple viral targets. *J. Virol.* **81**, 3005–3008 (2007).
42. Zahid, M.N. *et al.* The post-binding activity of scavenger receptor BI mediates initiation of hepatitis C virus infection and viral dissemination. *Hepatology* **57**, 492–504 (2013).
43. Fofana, I. *et al.* A novel monoclonal anti-CD81 antibody produced by genetic immunization efficiently inhibits hepatitis C virus cell-cell transmission. *PLoS ONE* **8**, e64221 (2013).
44. Jilek, B.L. *et al.* A quantitative basis for antiretroviral therapy for HIV-1 infection. *Nat. Med.* **18**, 446–451 (2012).
45. Iwami, S. *et al.* Quantification system for the viral dynamics of a highly pathogenic simian/human immunodeficiency virus based on an in vitro experiment and a mathematical model. *Retrovirology* **9**, 18 (2012).

Supplementary information accompanies this paper on the *CPT: Pharmacometrics & Systems Pharmacology* website (http://www.wileyonlinelibrary.com/psp4)